

## Electronic Structure of Glassy Chalcogenides $\text{As}_4\text{Se}_4$ and $\text{As}_2\text{Se}_3$ : A Joint Theoretical and Experimental Study

Jun Li and D. A. Drabold

*Department of Physics and Astronomy, Condensed Matter and Surface Science Program, Ohio University, Athens, Ohio 45701-2979*

Sumi Krishnaswami, Gang Chen, and Himanshu Jain

*Department of Materials Science & Engineering, Lehigh University, 5 East Packer Avenue, Bethlehem, Pennsylvania 18015-1539*

(Received 9 August 2001; published 14 January 2002)

We present an interpretation of the x-ray absorption spectra of arsenic chalcogenide glasses,  $\text{As}_4\text{Se}_4$  and  $\text{As}_2\text{Se}_3$ , from a first-principles calculation. Our calculation identifies the atomistic origins of the observed photoemission data. The importance of structural “building blocks” present in a particular glass to the electron states is emphasized. The effects of disorder on the electronic spectra are clearly demonstrated by a significant change in the electronic density of states, originating in the breakdown of long-range order coherence in the bonding states of the building blocks. We discuss the relation between observed *in situ* light-induced changes and the electronic structure.

DOI: 10.1103/PhysRevLett.88.046803

PACS numbers: 73.61.Jc, 71.23.-k, 82.80.Pv, 71.20.-b

Arsenic selenide glasses are heavily studied materials because of their unique light-induced effects [1]. Recent novel phenomena observed on glassy (*g*-)  $\text{As}_4\text{Se}_4$  and  $\text{As}_2\text{Se}_3$  have opened a new area of inquiry into the topological structure, dynamics, and electronic structure of these glasses. Krecmer *et al.* [2] demonstrated an optomechanical effect in *g*- $\text{As}_4\text{Se}_4$  films, in which an optical signal was directly converted into mechanical strain without the traditional combination of electro-optic and piezoelectric effects. Hisakuni and Tanaka [3] observed the electronic nature of the fascinating *athermal* photomelting in *g*- $\text{As}_2\text{Se}_3$ . But little knowledge of the electronic structure in the glassy forms has been accumulated. Recently, we have proposed two chalcogenide glass models, for *g*- $\text{As}_4\text{Se}_4$  and *g*- $\text{As}_2\text{Se}_3$ , and made a detailed comparison of their structural features [4]. Encouraging qualitative agreement with the existing experimental photoemission spectra [5] was obtained for our *g*- $\text{As}_2\text{Se}_3$  model [6]. The appearance of accurate x-ray photoemission spectrum (XPS) measurement on *g*- $\text{As}_4\text{Se}_4$  [7] made a fairly direct precise comparison between the experiment and calculation possible.

In this Letter, we present a calculation of the electronic structure of models of *g*- $\text{As}_4\text{Se}_4$  using the first-principles program FIREBALL96 [8], which quantitatively predicts the observed features in the experimental photoemission spectrum, while agreeing with structural and vibrational measurements [4,6]. This Hamiltonian employs four essential approximations: (1) nonlocal, norm-conserving pseudopotentials; (2) the Harris functional; (3) the local density approximation (LDA) within the density functional theory; and (4) a minimal basis of one *s* and three *p* orbitals per site. For a thorough discussion, see Ref. [8]. The minimal basis set tends to compensate the usual LDA underestimate of the gap, commonly producing an optical gap near experiment. For the valence states discussed here, use of this

Hamiltonian is well justified; for unoccupied states basis incompleteness would be a relevant issue.

The calculated electronic density of states (DOS) of *g*- $\text{As}_4\text{Se}_4$  is shown in Fig. 1a along with the recent high accuracy photoemission measurements of Krishnaswami *et al.* [7]. The experiment on *g*- $\text{As}_4\text{Se}_4$  was obtained by using XPS measurement on as-prepared  $\text{As}_4\text{Se}_4$  films with an energy increment of 0.05 eV for the spectrum. The valence band exhibits two broad features. The lowest band between  $-15$  and  $-7$  eV originates from the atomic *s*-like states of As and Se. The next band contains *p*-like bonding states lying between  $-6.0$  and  $-2.23$  eV and predominately *p*-like nonbonding states in the topmost valence region (lone pairs band in nature). These identifications agree with general expectations about the electronic structure of chalcogenide materials. The electronic spectra of *g*- $\text{As}_2\text{Se}_3$  also yields fair agreement in Fig. 1b. Even without the transition matrix elements, the widths, positions and number of peaks in the *p* band are in good quantitative agreement with experiments. This suggests a rather weak energy dependence in these matrix elements.

The characteristic of the *p* band in arsenic selenide glasses is represented by three distinct groups of peaks as indicated in the spectra of Fig. 1. The first group (I) contains all the bonding states whose energies (in eV) fall within  $[-6.0, -3.66]$ . The second group (II) includes the bonding states with energies in  $[-3.66, -2.23]$ . The last group (III) is the lone pairs states in the topmost region of  $[-2.23, 0.0]$ . Since the lone pair nature of group III has been widely accepted, we will focus on the understanding of the bonding states in intervals I and II.

We begin by examining the charge distribution of states on a main building block [4],  $\text{As}-\text{AsSe}_2$ , in *g*- $\text{As}_4\text{Se}_4$ . The bond charge shown in Fig. 2 is obtained by summing states of groups I and II and mapping it onto the Se-As-Se plane. One notices immediately that group I represents

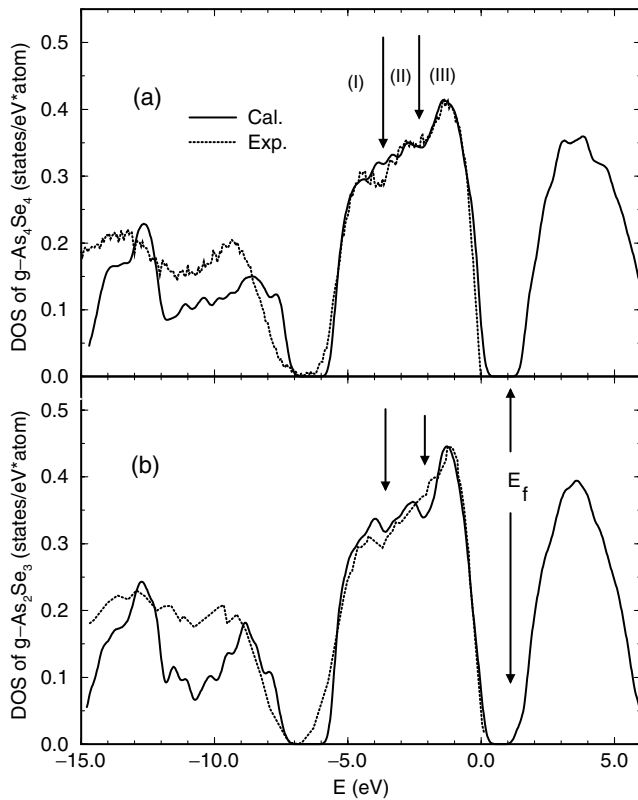


FIG. 1. Comparison between experimental and calculated electronic DOS for (a)  $g\text{-As}_4\text{Se}_4$  and (b)  $g\text{-As}_2\text{Se}_3$ . The calculated top of the valence band is set to zero. In order to facilitate comparison, the spectra were aligned at the highest point of the valence band. The calculated electronic spectra were broadened by the experimental resolution. Three different groups of peaks (I, II, and III) in the  $p$  band become clear from the distinct valley separating each.

states involved in intrablock bonding. The charge is confined largely within the perimeter of the building blocks. In contrast, the charge of group II is displaced out of the block and extends into the “interstitial” regions between neighboring building blocks. The nature of the bonds in group II can be attributed to the interblock bonding. Further inspection indicates that the difference of bonding between groups I and II is essentially the same for other building blocks in  $g\text{-As}_4\text{Se}_4$  and  $g\text{-As}_2\text{Se}_3$ . Thus we interpret the observed three groups of peaks in Fig. 1 to be intrinsically due to the intrabuilding and interbuilding block bonds and lone pairs.

It is not difficult to understand the energy ordering from group I to group III. The intrablock bonds, lying the lowest in energy, experience the strongest potential. On the other end, the local nature of lone pairs makes states of group III efficiently isolated from effective interaction, shifting them to the topmost valence region. Between them, the bonding states of group II extend between building blocks receiving an intermediate interblock interaction. Based on this understanding, we believe that the bonding characteristic of group I through group III should be a general feature

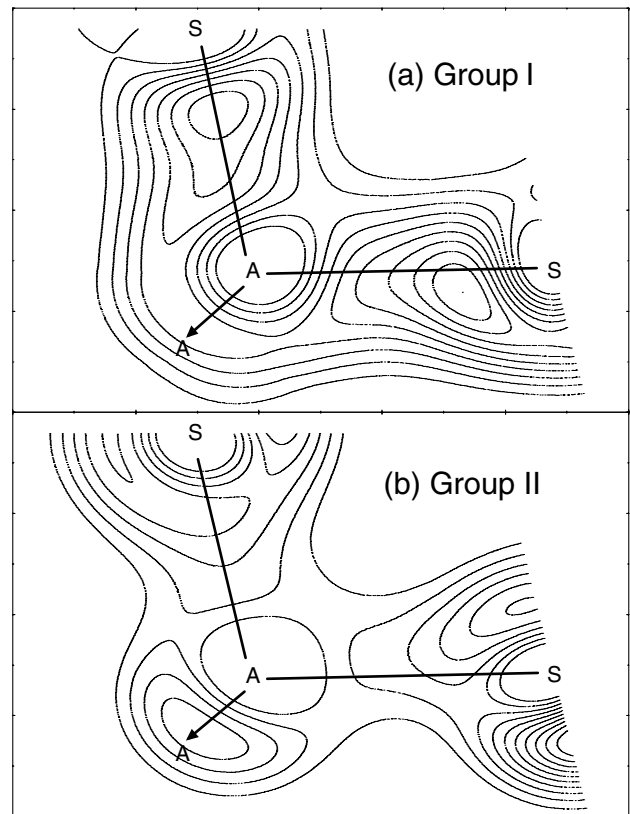


FIG. 2. Bond charge around a main building block,  $\text{As-AsSe}_2$ , of  $g\text{-As}_4\text{Se}_4$ . The charge contours are summed from states of (a) group I in  $[-6.0, -3.66]$  eV and (b) group II in  $[-3.66, -2, 23]$  eV as indicated in Fig. 1. Here A stands for As and S for Se. The arrows indicate the As-As bonds pointing below the mapping plane. Note that the dense contour along the arrow in (b) is thus above the As-As bond.

for chalcogenide materials in both glassy and crystalline forms.

To trace the effects of disorder on the electronic structure, we examine the systematic changes of electronic signatures of similar building blocks between the crystals and the glasses. Since the topology of the pyramidal building block  $\text{AsSe}_3$  is simpler than  $\text{As-AsSe}_2$ , it is advantageous to begin with the main configuration of  $\text{As}_2\text{Se}_3$ . Figure 3 shows the projected electronic DOS of the same configuration,  $\text{AsSe}_3$ , in  $c\text{-As}_2\text{Se}_3$  and  $g\text{-As}_2\text{Se}_3$  along with the further projection on the individual elements As and Se. The calculation of  $c\text{-As}_2\text{Se}_3$  and  $c\text{-As}_4\text{Se}_4$  was performed on the reported crystalline structure [9] by the same program, FIREBALL96 [10]. The crystalline electronic DOS was integrated over 29 K points in the irreducible part of the Brillouin zone.

The bonding characteristic of  $\text{AsSe}_3$  is essentially the same in  $c\text{-As}_2\text{Se}_3$  and  $g\text{-As}_2\text{Se}_3$ . Because of the layered structure in the crystalline form, the intrablock bonds develop into the intralayer bonds and the interblocks bonds evolve into the interlayer bonds of  $c\text{-As}_2\text{Se}_3$ . The identification of the intralayer and interlayer bonds is coincident

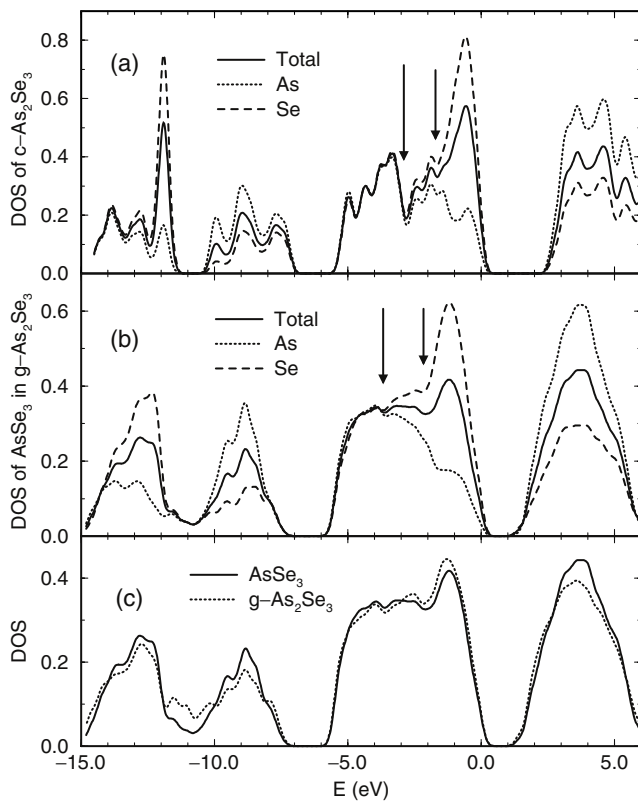


FIG. 3. Comparison of the electronic DOS of the configuration,  $\text{AsSe}_3$ , in (a)  $c\text{-As}_2\text{Se}_3$  and (b)  $g\text{-As}_2\text{Se}_3$  along with the projected DOS on elements As and Se. The arrows indicate the valleys where the spectra change charge distribution. However, the distinction is easier to be observed between groups I and II than between groups II and group III. The width of group I shrinks from crystal to glass and the width of groups II and III are increased. In (c) the electronic DOS of  $\text{AsSe}_3$  is compared to the same total DOS of  $g\text{-As}_2\text{Se}_3$  in Fig. 1b to show the contribution from other building blocks of  $g\text{-As}_2\text{Se}_3$ .

with a previous calculation [11]. The identification is similar for the configuration of  $\text{As-AsSe}_2$  in  $c\text{-As}_4\text{Se}_4$  and  $g\text{-As}_4\text{Se}_4$ . Since  $c\text{-As}_4\text{Se}_4$  is a molecular crystal, the bonding states of group I are made up from the intramolecule bonds and those of group II by the intermolecule bonds according to current calculation.

Along with the evolution of the individual building block bond in glasses into the collective bond in crystals, the electronic spectra undergo an essential change as demonstrated in Figs. 3a and 3b. The spectrum of glass is quite featureless in each bonding range, in contrast to the obvious substructures in the spectrum of crystal, which is due to the long-range coherence breaking down in the glassy form. Furthermore, the valleys, which distinguish the three groups in Fig. 3, change positions from crystal to glass, indicating that the disorder pushes more electrons into the interstitial region, thus increasing the width of group II and reducing the range of group I. This may correspond to the fact that the glass has a lower density or a larger interstitial interface than the crystal.

The significance of the three groups is also demonstrated by the representative charge distribution on As and Se. As shown in Figs. 3a and 3b, the projected DOS on Se closely converges to that on As in the group I region for both  $c\text{-As}_2\text{Se}_3$  and  $g\text{-As}_2\text{Se}_3$ . The bonding charge of group I tends to equally distribute on As and Se as indicated by Table I. For group II, Se slightly gains electrons from As, in contrast to the equal distribution tendency in group I (Table I). In group III, the charge on Se dominates As. However, it is quite clear from Fig. 3 that the bonding states of group II project a tail into the lone pair region of group III, making an absolute separation on the energy scale of different bonding states impossible. Even though the charge concentrates on Se, some charge localizes on As in the group III region as shown in Table I.

Other structural configurations are found to make a larger contribution to group II and group III rather than to group I as indicated by Fig. 3c. Interaction between building blocks strongly affects the states extending into the interstitial regions. Then the interblock bonds become sensitive to the local relative orientation between building blocks. The intrablock bonds are more likely to be dependent upon the short-range order instead of the long-range order. Thus the change is quite small for intrablock bonds. We conclude that group II is a representative region of the disorder effects. The conduction bands of  $g\text{-As}_4\text{Se}_4$  and  $g\text{-As}_2\text{Se}_3$  are lower than those of crystals, agreeing with the general observation that the gap of glasses is softer and narrower than the corresponding crystals. Near the gap region, another significant contribution originates from the miscoordinated atoms, as proposed by the valence alternation pair (VAP) [12–14] theory. The states at the top of the valence band in the glasses are from the under-coordinated Se and As, and the states in the bottom region of the conduction band are from the over-coordinated Se and As. The concentration of Se-based VAP's dominate the As coordination defects in both models [4].

Since any light-induced structural change is likely to involve the bond charge between different building blocks [4], the above understanding of the bonding states in different materials helps to explain the photoresponse in recent *in situ* experiments on  $g\text{-As}_2\text{Se}_3$  and  $g\text{-As}_4\text{Se}_4$ . Chen *et al.* [15] have found that, under *in situ* laser irradiation, the Se-Se defect bonds were the primary atomic configuration showing light-induced structural changes. This may correspond to the Se-based self-trapped exciton effects proposed by Fritzsche [16]. In this model an intimate VAP constitutes a self-trapped exciton and can move apart by a further bond-switching reaction to become random VAP's. This mechanism has been demonstrated in our recent simulation on  $g\text{-As}_2\text{Se}_3$  [17], in which, however, we discussed the As-based self-trapped exciton process. Se-based VAP's also undertook this process. We believe that this "VAP type" of photo response should be connected with the direct band-gap or subband-gap

TABLE I. Averaged total bond charge around the main configuration for states in groups I, II, and III. Note that the range of the three groups is different in crystals. For  $c$ -As<sub>2</sub>Se<sub>3</sub>, I<sub>ε</sub>(-5.5, -2.8) eV, II<sub>ε</sub>(-2.8, -1.64) eV, and III<sub>ε</sub>(-1.64, 0) eV. The corresponding ranges for  $c$ -As<sub>4</sub>Se<sub>4</sub> are (-5.8, -3.2) eV, (-3.2, -1.3) eV, and (-1.3, 0) eV, respectively. The classification is based on the spectral behavior as indicated in Fig. 3.

	$g$ -As <sub>2</sub> Se <sub>3</sub>		$g$ -As <sub>4</sub> Se <sub>4</sub>		$c$ -As <sub>2</sub> Se <sub>3</sub>		$c$ -As <sub>4</sub> Se <sub>4</sub>	
	As	Se	As	Se	As	Se	As	Se
I	1.130	1.058	0.991	1.056	1.452	1.446	1.165	1.335
II	0.886	1.062	0.872	1.087	0.590	0.756	1.284	1.570
III	0.723	2.021	0.999	1.968	0.690	1.976	0.436	1.211

illumination induced structural changes. Significantly, Krishnaswami *et al.* [7] found a depletion of states in the group II region as a result of the *in situ* irradiation on the  $g$ -As<sub>4</sub>Se<sub>4</sub> film in air. They have explained it as the light-induced depletion of As-As bonds and reaction with oxygen. Considering the characteristic of the states in group II, we tentatively propose another possible interpretation. Since the As-O bonds may form only up to a limited depth near the surface [7], the oxygen may behave as an interstitial impurity between the building blocks. The oxygen absorbs the charge lying between the building blocks, which originally belonged to the interblock bonds of group II. Meanwhile, the states in group II have the charge transfer feature, the high electronegativity of oxygen gained more charge from As, making a significant depletion of the states in the As-based bonds. On the other hand, the states in group I and group III localize either on the intrabuilding blocks or atomic sites and receive less charge from the interstitial oxygen. We have found that the oxygen can introduce localized gap states, which should enhance the gap/subgap absorption in air. Further simulation to distinguish the oxygen's role is in progress.

In this Letter, we report an interpretation of the observed structures in the experimental photoemission spectra, and show in microscopic detail the origin of these spectra. We demonstrated a significant difference between the crystalline and the glassy forms in the electronic spectra. The disorder affects the electronic structure by breaking the long-range coherence in the arrays of the building blocks. Previous experimental efforts to compare the electronic structure of the crystalline and the glassy As<sub>2</sub>S<sub>3</sub> and As<sub>2</sub>Se<sub>3</sub> using the spectra of optic reflectivity revealed remarkably small effects from disorder on the electronic spectra [18]. The XPS provides direct information about all the valence bands and is widely employed to directly compare with the theoretical work. The different charge characteristic in the groups of bonding states may be helpful to understand the light-induced structural or chemical changes.

This work was supported in part by the National Science Foundation under Grant No. DMR 00-81006 and a Focused Research Group Grant No. DMR 00-74624.

J. Li thanks Dr. Cecilia Noguez for helpful communication of the crystalline coordinates.

- [1] For example, K. Shimakawa, A. Kolobov, and S. R. Elliott, *Adv. Phys.* **44**, 475 (1995).
- [2] P. Krecmer, A. M. Moulin, R. J. Stephenson, T. Rayment, M. E. Welland, and S. R. Elliott, *Science* **277**, 1799 (1997).
- [3] H. Hisakuni and K. Tanaka, *Science* **270**, 974 (1995).
- [4] Jun Li and D. A. Drabold, *Phys. Rev. B* **64**, 104206 (2001).
- [5] K. S. Liang, *J. Non-Cryst. Solids* **18**, 197 (1975).
- [6] Jun Li and D. A. Drabold, *Phys. Rev. B* **61**, 11998 (2000).
- [7] S. Krishnaswami, H. Jain, and A. C. Miller, ANC Workshop at Bucharest, 2001.
- [8] O. F. Sankey and D. J. Niklewski, *Phys. Rev. B* **40**, 3979 (1989); A. A. Demkov, J. Ortega, O. F. Sankey, and M. Grumbach, *Phys. Rev. B* **52**, 1618 (1995).
- [9] A. A. Vaipolin, *Sov. Phys.-Crystallogr.* **10**, 509 (1966); A. L. Renninger and B. L. Averbach, *Acta Crystallogr. Sect. B* **29**, 1583 (1973).
- [10] We can make a detailed examination on the precision and reliability of FIREBALL96 on the crystalline calculation. The electronic DOS of  $c$ -As<sub>2</sub>Se<sub>3</sub> is consistent with the existed first-principles pseudopotential calculation [11]. We also performed additional calculation on both  $c$ -As<sub>4</sub>Se<sub>4</sub> and  $c$ -As<sub>2</sub>Se<sub>3</sub> using the full-electronic, self-consistent linearized augmented plane-wave method: Jun Li, Chun-gang Duan, Zong-quan Gu, and Ding-sheng Wang, *Phys. Rev. B* **57**, 6925 (1998). The results of FIREBALL96 do reasonably agree with the other first-principles calculation on the band structures and the characteristic of the bonding states.
- [11] Eugen Tarnow, A. Antonelli, and J. D. Joannopoulos, *Phys. Rev. B* **34**, 4059 (1986).
- [12] P. W. Anderson, *Phys. Rev. Lett.* **34**, 953 (1975).
- [13] R. A. Street and N. F. Mott, *Phys. Rev. Lett.* **35**, 1293 (1975).
- [14] Marc Kastner, David Adler, and H. Fritzsche, *Phys. Rev. Lett.* **37**, 1504 (1976).
- [15] Gang Chen, Himanshu Jain, Syed Khalid, Jun Li, David Drabold, and Stephen R. Elliott, *Solid State Commun.* **120**, 149 (2001).
- [16] H. Fritzsche, *Philos. Mag. B* **68**, 561 (1993).
- [17] Jun Li and David Drabold, *Phys. Rev. Lett.* **85**, 2785 (2000).
- [18] R. Zallen, R. E. Drews, R. L. Emerald, and M. L. Slade, *Phys. Rev. Lett.* **26**, 1564 (1971).